Characteristics of Top-Gate Polysilicon Thin-Film Transistors Fabricated on Fluorine-Implanted and Crystallized Amorphous Silicon Films

Chien Kuo Yang, Tan Fu Lei, and Chung Len Lee

Department of Electronics Engineering, National Chiao Tung University, Hsinchu, Taiwan

ABSTRACT

This paper presents a comprehensive study on the characteristics of n- and p-channel polycrystalline-silicon (polysilicon) thin-film transistors (TFTs) fabricated on fluorine-implanted-then-crystallized amorphous silicon films. Amorphous silicon films of two thicknesses were implanted with different energies and various dosages of fluorine, and studied using transmission electron microscopy (TEM) and secondary-ion mass spectrometry (SIMS). The electrical characteristics of TFTs fabricated on the films were correlated with the results of TEM and SIMS. It was found that field-effect mobilities of both n- and p-channel devices were improved by the fluorine implantation thanks to the enhanced grain size and the fluorine passivation effect. For the p-channel device, the fluorine implantation did not improve the subthreshold swing and even degraded it after hydrogenation. This result was thought to be caused by the fluorine-induced negative charges in oxides. However, a thin active layer and a deep implantation reduced this degradation.

In 1980 Kamins *et al.*[1] were the first to suggest that fluorine be used to passivate grain boundaries of the polysilicon TFT. The concept was not realized until 1991, however, when fluorine ion implantation (FII) was used to incorporate fluorine into the poly-Si TFT[2] and studies indicated an improvement in device performance. Recently, other studies have further examined the effects of FII on the polysilicon TFT.[3-5] For example, Chern *et al.*[3] studied the passivation effects of fluorine on polysilicon thin-film transistors by implanting different doses of fluorine into the device channel. Generally, FII was applied to the polysilicon TFT in two ways, *i.e.*, fluorine was implanted after the amorphous-silicon (α-Si) crystallization,[3,4] or before the α-Si crystallization.[5] For FII applied after the α-Si crystallization, the fluorine had demonstrable passivation effects on the polysilicon TFT to improve device performance.[1-3] Moreover, because of the fluorine incorporation, negative charges were induced in the oxide under the offset region of the bottom-gate TFT, creating an LDD-like structure to further improve the TFTs ON- and OFF-currents.[4] In the above reports on FII applied after the α-Si crystallization, the grain regrowth effect of the amorphized film was not considered, even though high implantation doses and energies were used.[6] A recent study on FII before the α-Si crystallization reported that fluorine implantation with high doses and deep projection-ranges, like silicon implantation, could also enhance the grain sizes of, but have no passivation effects on, the polysilicon.[5] The same study also reported that fluorine was a hole generator in the recrystallized polysilicon films. However, this study[5] showed inconsistent results between material properties and electrical characteristics (*e.g.*, a larger grain-size TFT but a lower ON-current), and electrical characteristics were not characterized completely (*e.g.*, without p-channel devices).

In this work, FII applied to as-deposited α-Si films to fabricate TFTs was thoroughly studied. Fluorine of different doses and energies were implanted into α-Si of two thicknesses, n- and p-channel polysilicon TFTs were fabricated, and their electrical properties were discussed in detail. At the same time, the hydrogen passivation effect on the fabricated TFTs was also studied. Transmission electron microscopy (TEM) and secondary-ion mass spectrometry (SIMS) were used to investigate the implanted α-Si which received different thermal treatments, including low-temperature (550°C) crystallization and high-temperature (850°C) oxidation and annealing. It was found that the improved electrical characteristics could be attributed to both the enhanced grain size by FII and the fluorine's own passivation effect. Moreover, the fluorine-induced negative charges in oxides were thought to be the reason for the degradation of the p-channel device's subthreshold swing.

Experimental

At first, undoped α-Si films of two thicknesses, approximately 100 and 60 nm, were deposited on thermally oxidized silicon wafers at 550°C by a low-pressure chemical vapor deposition (LPCVD) system. These films were then implanted by fluorine. For the thicker films, the implantation energy was 30 keV and the dose varied from 8×10^{14} cm^{-2} to 3×10^{15} cm^{-2}. For the thinner films, the implantation energies were 5, 15, and 30 keV with a dose of 2×10^{15} cm^{-2}. These wafers then were annealed at 600°C for 45 h to transform the α-Si films into polycrystalline films. After active islands were defined, a 28 nm gate oxide was grown in dry O_2 at 850°C. Another 300 nm polysilicon film was deposited at 625°C by the LPCVD system to be the gate electrode. Self-aligned As and BF_2^+ implantations of a dose of 5×10^{15} cm^{-2} were performed to form the source and the drain and to dope the gate electrodes for the n- and p-channel devices, respectively. The implantation energies are 65 and 40 keV for 100 and 60 nm polysilicon films, respectively. The dopants were activated at 850°C for 30 min in an N_2 ambient. Some samples were subjected to the H_2/N_2 plasma treatment in a commercial plasma-enhanced chemical vapor deposition (PECVD) system at 300°C for 1 h. All devices were then capped with a 360 nm PECVD SiO_2. The total pressure was 800 mTorr, the RF power was 10 W, and the deposition rate was 60 nm/min. Finally, after contact holes were opened, Al was deposited, patterned, and then sintered at 300°C. During the above process, control devices without the fluorine implantation were also fabricated for comparison. All the devices, with and without the fluorine implantation, were pretreated by a diluted HF solution without a water rinse and immediately spun dry just before their gate-oxide growth. The diluted HF treatment was denoted as DHF.

Results and Discussion

100 nm poly-si film devices.—Figure 1a and b shows the TEM micrographs, including the diffraction patterns and the dark-field images, of the poly-Si films without FII, and with 3×10^{15} cm^{-2} FII, respectively. The grain size of the FII film was effectively enhanced as compared to the unimplanted film. The diffraction pattern of the FII film also shows how the FII film had crystallized more than the film without FII. This contradicts the report by Park *et al.*,[5] which showed no increase of the grain size of the poly-Si film, even when the fluorine implantation exceeded 5×10^{15} cm^{-2}.

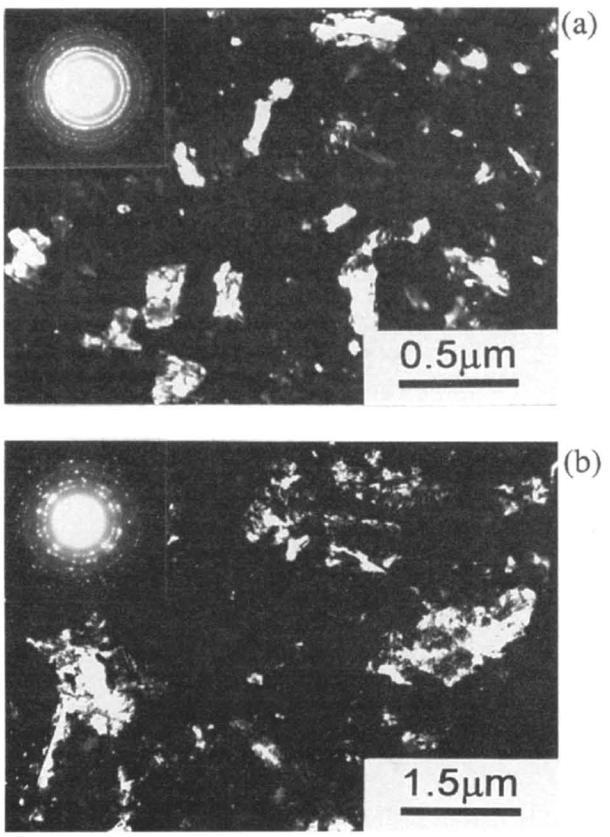

Fig. 1. The TEM micrographs, including diffraction pattern and dark-field image, of the samples with (a) no FII and (b) 3×10^{15} cm^{-2} FII.

Figure 2 shows the SIMS data on the fluorine distributions of the films with 1×10^{15} and 3×10^{15} F/cm^2 implantations, respectively. The implanted fluorine, after the following annealing and oxidation steps, had redistributed itself into the gate- and isolation-oxides, with most of them gathering at gate-oxide/poly-Si/SiO_2 interfaces. The original implanted fluorine peak disappeared and the 3×10^{15} cm^{-2} film had higher fluorine peaks at interfaces, yet it had the same distribution as that of the 1×10^{15} cm^{-2} film at the polysilicon bulk.

Figure 3 shows the drain currents, before hydrogen passivation, as a function of the gate voltage of n- and p-channel TFTs fabricated on poly-Si films with various FII doses. Figure 4a and b shows the values of the electrical parameter of the ON-state current, the field effect mobility, the subthreshold swing, and the threshold voltage plotted as a function of the implantation dose, for n- and p-channel TFTs, respectively. These figures show that, (*i*) FII improved the device characteristics for both the n- and p-channel TFTs and (*ii*) the greater the implanted dose, the greater the improvement, except for the OFF-state current. The improvement was not significant, however, until the dose was increased to at least 3×10^{15} cm^{-2}. Also, compared with the n-channel devices, the p-channel devices had different subthreshold characteristics. Obviously it was the grain-size enhancement, caused by the fluorine implantation, that improved the device characteristics. However, in addition to that, some other mechanisms could also have played roles in affecting the device characteristics; examples could be the enhanced OFF current or the different subthreshold characteristics between n- and p-channel devices. One such mechanism could be that fluorine acted as a hole generator in recrystallized polysilicon films because of its large electron-negativity,[5-9] which would lead to p-channel devices being in the accumulation mode and n-channel devices in the inversion-mode.[10] This made p-channel devices switch on more easily than did n-channel devices. Nevertheless, in Fig. 2, it was observed that more fluorine accumulated at the Si/SiO_2 interface than at the bulk of poly-Si. It is believed that it was the fluorine at the Si/SiO_2 interface, rather than at the polysilicon bulk, that increased the OFF-state current. Hence, another possible mechanism considered was the double-gate effect caused by the negative fixed charges induced by fluorine incorporated in oxides.[12] The negative fixed oxide charges caused positive flatband shifts. Therefore, for the top-gate, the turn-on voltage of the top channel was shifted to the positive. In addition, an induced back-channel caused by the negative charges in the isolation oxide occurred. This affected both the drain leakage current and the subthreshold characteristic.[13,14] For n-channel FII devices, the enhanced negative bias on the top-gate and the additional negative bias on the bottom-gate increased the electrical field at the drain junction; this increased field in turn led to the increased anomalous leakage current. The drain junction leakage was the main source of the anomalous leakage current, *i.e.* the OFF current, for TFTs.[15] For p-channel FII devices, due to the negative charges, the top and back channel might be still slightly ON until the top-gate bias is positive enough.

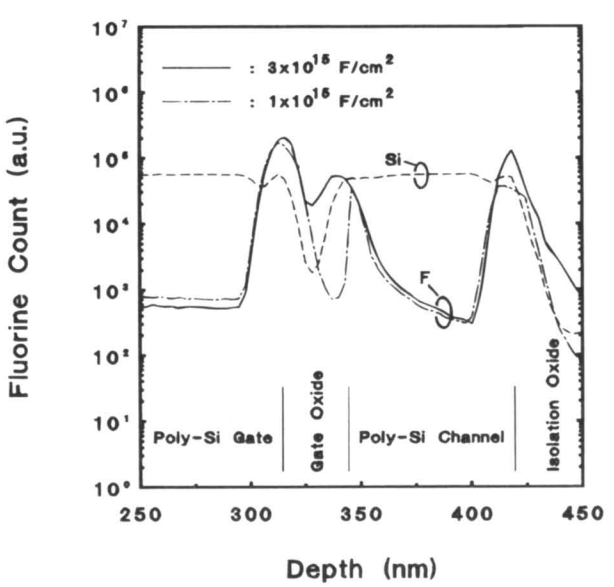

Fig. 2. The SIMS profiles of the samples with 1×10^{15} and 3×10^{15} F/cm^2 implantations, respectively.

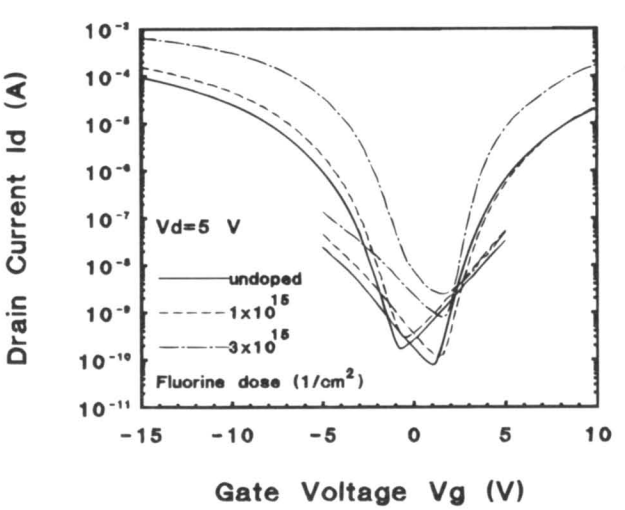

Fig. 3. The drain current, before hydrogen passivation, as a function of gate voltage for the devices with various FII doses.

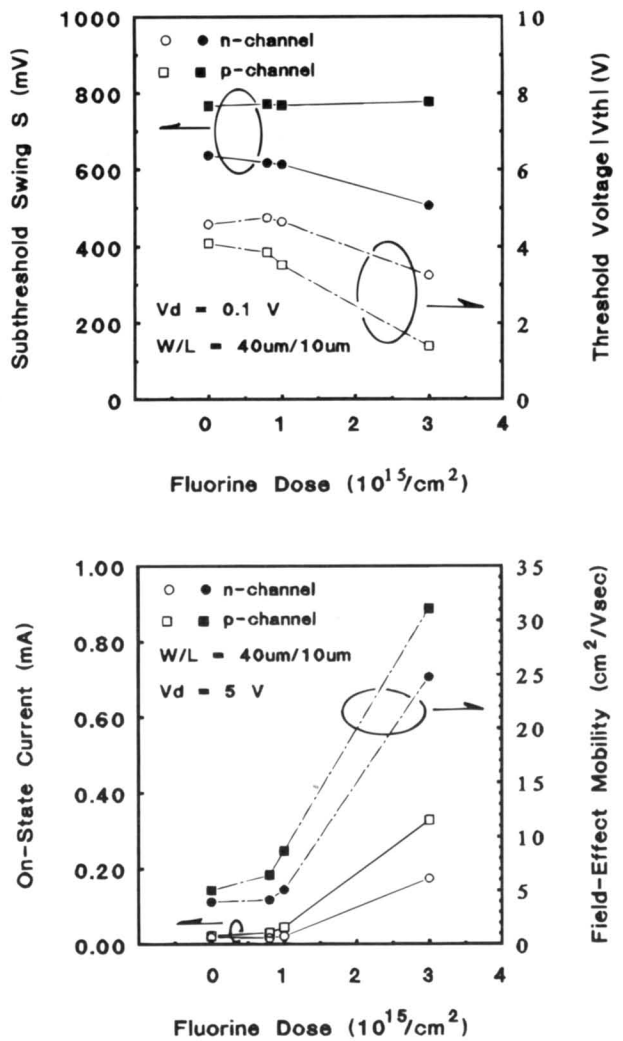

Fig. 4. The electrical parameters, including (a, top) subthreshold swing and threshold voltage and (b, bottom) field-effect mobility and ON-state current as a function of implantation dosage.

The above leakage current can be reduced effectively if a thinner polysilicon film is used; this issue is discussed later.

60 nm poly-Si film devices.—Figure 5 shows TEM micrographs, including diffraction patterns and dark-field images, for samples without FII (a) and implanted with fluorine at 15 (b) and 30 keV (c). The dosage of FII was 2×10^{15} cm^{-2} and the film thickness was 60 nm. For samples implanted at 15 keV and having the projected implantation range of about 30 nm, the grain size was only slightly than that of the control sample. However, for the 30 keV sample, with the projected implantation range slightly larger than 60 nm, the grain size was much enhanced. These results are similar to those reported by Park *et al.*[5] Hence, in order to increase the recrystallized grain size effectively, the implantation range should fall at the interface of the poly-Si film and the bottom isolation oxide. In addition, the grain size of the 30 keV sample in this section was smaller than that of the sample in Fig. 1. This was mainly because the 30 keV sample had a thinner poly-Si film which limited grain-growth.

Figure 6a-c shows the fluorine distributions of samples with three different implantation energies, *i.e.*, 5, 15, and 30 keV, respectively, and the distributions of the control sample which did not receive any FII but still received diluted HF (DHF) acid treatment. For these three implantation energies, the projected implantation peaks were at the top, the middle, and the bottom of the poly-Si films,

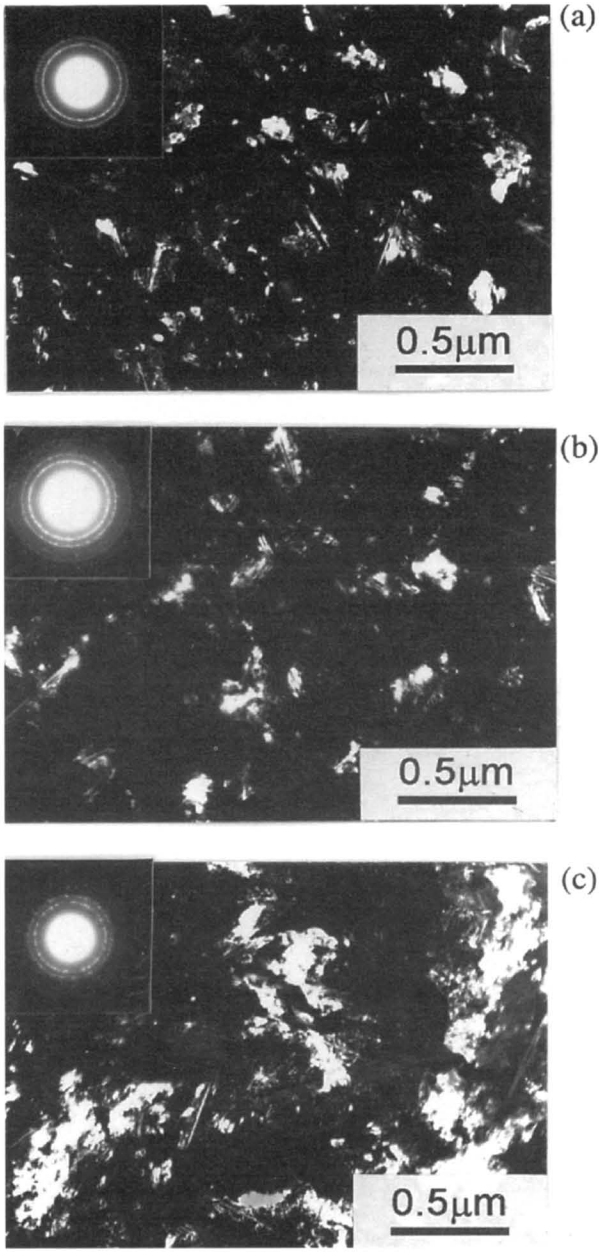

Fig. 5. The TEM micrographs, including diffraction pattern and dark-field image, of the samples with different implantation energies: (a) control, (b) 15 keV, and (c) 30 keV.

respectively. Due to the subsequent annealing and oxidation processes, most of the fluorine redistributed itself into the gate- and isolation-oxides or on the curves, and so the original peaks did not exist. However, the larger the implantation energy, the higher the fluorine peak at the bottom poly-Si/SiO_2 interface. Likewise the DHF control sample had a peak at the gate-oxide and the 5 keV sample gave a similar fluorine distribution near the gate-oxide/poly-Si interface as compared to the DHF control sample. This indicates that the DHF treatment also incorporated a significant amount of fluorine into its devices.

Figure 7 shows the drain current, before hydrogen passivation, as a function of the gate voltage for devices with various FII energies. Interestingly, I-V improvements were obtained by FII, even for the 5 keV sample. This contrasts reports from Park *et al.*,[5] where FII did not effectively improve I-V. The 30 keV device had the best electrical characteristics due to its largest grain size; its only flaw was a slightly increased OFF-state current. The slightly increased OFF-state current, similar to that of the 100 nm device, probably came from the many fluorine-induced

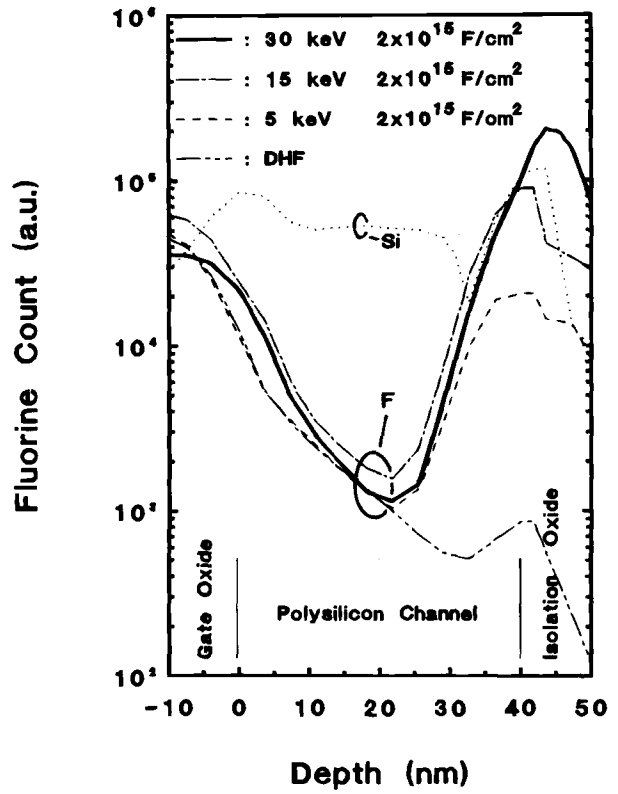

Fig. 6. The SIMS profiles of the samples with different implantation energies and the control without FII.

charges in the oxides. However, compared to the 100 nm device, the 30 keV device's leakage-current was lower due to the smaller thickness of the active layer.[13] As for the 15 keV device, although its grain size was not increased significantly, it still apparently improved electrical properties. This improvement is believed to stem from the combination of the grain size effect and the passivation effect of fluorine which resided in the film after crystallization. Park *et al.*[5] reported that although FII significantly enlarged grain size, little I-V improvement was found even for the sample implanted with fluorine at a high dose (4×10^{15} cm^{-2}) and a high implantation energy (60 keV). The 5 keV device was quite different, however: since the implantation damage was not severe and the implanted fluorine outdiffused during the crystallization stage, the characteristic improvement was minimal and indeed almost the same as that of the control sample.

Figure 8a shows the parameter values of the ON-state current and field-effect mobility while Fig. 8b gives the subthreshold swing and threshold voltage: all four values are expressed as a function of the implantation energy for the corresponding devices of Fig. 7. All cases demonstrated that the higher the implantation energy, the greater the improvement of the driving ability, the threshold voltage, and the subthreshold swing. Figure 8b clearly shows that the improvements on subthreshold swings of n- and p-channel devices were similar. This differed from that of the 100 nm devices of the first section, where improvement for the 3×10^{15} cm^{-2} p-channel device was not obtained. Because the 60 nm device was fabricated on thinner polysilicon layer, its subthreshold characteristic could be more effectively controlled by the top gate and the OFF-state current was reduced despite the existence of the induced back channel.[13]

Hydrogen passivation effect.—Figure 9 shows the subthreshold-swings as a function of (a) the fluorine dose for 100 nm poly-Si film devices and (b) the implantation energy for 60 nm poly-Si film devices after hydrogen passivation. Comparing the data in Fig. 9, 4b, and 8b showed that hydrogen passivation improved the subthreshold swings of all devices except for the 100 nm sample implanted with a dose of 3×10^{15} cm^{-2} at 30 keV in Fig. 9a. Figure 9a indi-

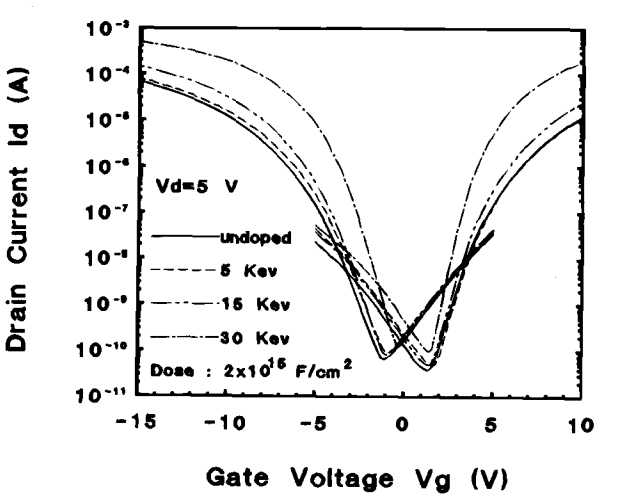

Fig. 7. The drain current, before hydrogen passivation, as a function of gate voltage for the devices with various FII energies.

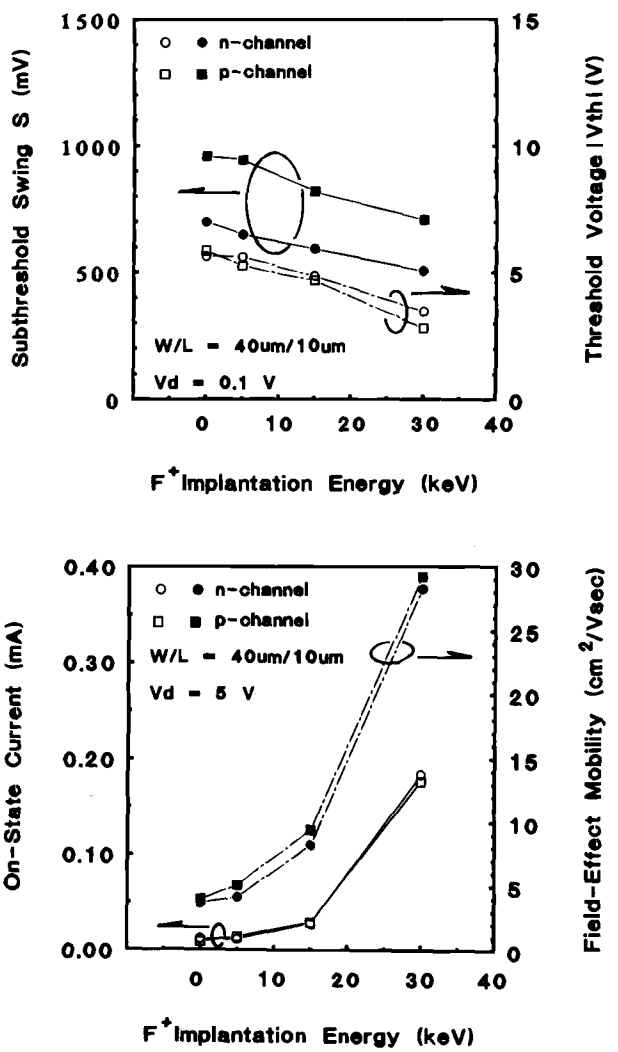

Fig. 8. The electrical parameters, including (a, top) subthreshold swing and threshold voltage, and (b, bottom) field-effect mobility and ON-state current as a function of implantation energy for the corresponding devices in Fig. 7.

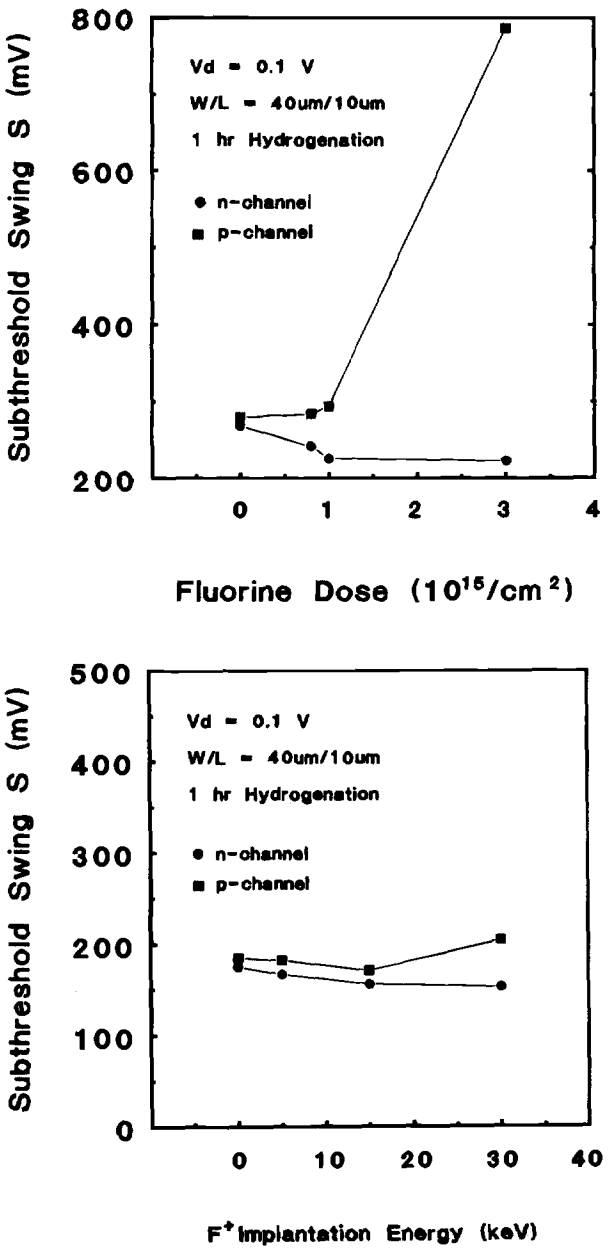

Fig. 9. The subthreshold-swing (*S*), after hydrogen passivation, as a function of (a, top) fluorine dose and (b, bottom) implantation energy, respectively.

cates that after hydrogen passivation the subthreshold-swing of the p-channel device was degraded, especially for the 3×10^{15} cm^{-2} case, as the fluorine dose increased. For the n-channel device, however, the subthreshold swing was improved further. These results could also be explained by the fluorine-induced negative charges at the isolation oxide (*i.e.*, bottom oxide). After hydrogen passivation, and because the trap-states were reduced more, the bottom channel, induced by the fluorine-induced negative charges, conducted more easily for the p-channel devices. The conducting back-channel made top-gate control of the drain-current less effective at the low top-gate bias, especially for the device with a thick active layer,[13] and then led to the increased of both the S factor and the OFF-state current. Thinning the active layer increased the controllability of the top-gate to the whole active layer and suppressed the back-channel effect. This explains why the S-factor of the 30 keV p-channel device of the 60 nm sample in Fig. 9b was not so seriously degraded as that of the 100 nm p-channel device in Fig. 9a. Another possible reason was that the 30 keV FII had more seriously damaged the bottom poly-Si/SiO_2 interface of the thin-film device. The damage could reduce the hole life time at the bottom surface,[16] so the back-channel did not conduct well.

The field-effect mobilities of the devices in Fig. 9, where they were hydrogen-passivation treated, are summarized in Table I with their process condition. For comparison, the mobilities of devices of a previous work[3] are also included. It is seen that hydrogen passivation further enhanced the field-effect mobilities of both the n- and p-channel devices. The DHF treatment, applied after crystallization but before gate-oxidation, gave field-effect mobilities comparable with those of the fluorine-implanted devices of 2×10^{15} cm^{-2} at 25 keV, and annealed at 850°C for 1 h.

Conclusions

This study systematically examined FII prior to α-Si crystallization and its effects on the TFTs fabricated on the FII poly-Si thin films. FII prior to α-Si crystallization improved the electrical characteristics of the TFT, with the improvement coming from both the grain size enhancement and the fluorine passivation effect. The higher the implantation dosage and energy, the greater the improvement. As hydrogenation was applied, further improvements on electrical characteristics, especially in field-effect mobility, were found. There was a negative charge effect, however, which was induced by the implanted fluorine at the gate as well as at the bottom oxides and which affected device characteristics, such as S and OFF-state current. This negative charge effect increased the p-channel TFT leakage and degraded S after hydrogenation. However, this condition could be reduced if the thickness of the active poly-Si film was decreased. Finally, it was found that applying the DHF process to the poly-Si film before it was subjected to gate oxidation introduced fluorine into TFTs to obtain the desired passivation effect.

Acknowledgment

This work was supported by the ROC National Science Council under Contract No. NSC-83-0404-E009-017.

Manuscript submitted Sept. 14, 1995; revised manuscripot received July 1, 1996.

The National Chiao Tung University assisted in meeting the publication costs of this article.

Table I. Summary of process conditions and field-effect mobilities after hydrogen passivation in this work and a previous report by Chern *et al.*[3]

Polysilicon thickness	Preimplantation preparation of films	Fluorine ion implantation	Anneal or crystallization	DHF	μ (cm^2/Vs) n-channel	μ (cm^2/Vs) p-channel
60 nm[a]	550°C α-Si, 600°C 20 h	—	—	No	12.0	10.8
60 nm[a]	550°C α-Si, 600°C 20 h	2×10^{15} cm^{-2} 25 keV	850°C 1 h	No	20.2	14.6
100 nm	550°C α-Si, —	—	600°C 45 h	Yes	18.0	16.4
100 nm	550°C α-Si, —	3×10^{15} cm^{-2} 30 keV	600°C 45 h	Yes	41.7	44.0
60 nm	550°C α-Si, —	—	600°C 45 h	Yes	20.1	12.8
60 nm	550°C α-Si, —	2×10^{15} cm^{-2} 30 keV	600°C 45 h	Yes	44.4	34.4

[a] See Ref. 3.

REFERENCES

1. T. I. Kamins and Marcoux, *IEEE Electron Device Letters*, **EDL-1,** 159 (1980).
2. H. Kitajima, Y. Suzuki, and S. Saito, *Tech. Dig. Solid State Dev. Mater.*, 174 (1991).
3. H. N. Chern, C. L. Lee, and T. F. Lei, *IEEE Trans. Electron Devices*, **ED-41,** 698 (1994).
4. S. Maegawa, T. Ipposhi, S. Maeda, H. Nishimura, T. Ichiki, M. Ashida, O. Tanina, Y. Inoue, T. Nishimura, and N. Tsubouchi, *ibid.*, **ED-42,** 1106 (1995).
5. J. W. Park, D. G. Moon, B. T. Ahn, and H. B. Im, *Thin Solid Films*, **245,** 228 (1994).
6. N. Yamauchi and R. Reif, *J. Appl. Phys.*, **75,** 3235 (1994).
7. M. Y. Tsai and B. G. Streetman, *ibid.*, **50,** 183 (1979).
8. I. W. Wu, A. Chiang, M. Fuse, L. Ovecoglu, and T. Y. Huang, *ibid.*, **65,** 4037 (1989).
9. C. G. van de Walle, F. R. McFeely, and S. T. Pantelides, *Phys. Rev. Lett.*, **61,** 1867 (1988).
10. S. D. S. Malhi, H. Shichijo, S. K. Banerjee, R. Sundaresan, M. Elahy, G. P. Pollack, W. F. Richardson, A. H. Shah, L. R. Hite, R. H. Womack, P. K. Chatterjee, and H. W. Lan, *IEEE Trans. Electron Devices*, **ED-32,** 258 (1985).
11. M. Y. Tsai, D. S. Day, B. G. Streetman, P. Williams, and C. A. Evans, Jr., *J. Appl. Phys.*, **50,** 188 (1979).
12. P. J. Wright and K. C. Saraswat, *IEEE Trans. Electron Devices*, **ED-36,** 879 (1989).
13. T. Hashimoto, T. Mine, T. Yamanaka, N. Hashimoto, A. Shimizu, T. Nishida, and Y. Kawamoto, *Tech. Dig. Solid State Dev. Mater.*, 393 (1990).
14. F. Hayashi, H. Ikeuchi, M. Kitakata, and I. Sasaki, *IEDM Tech. Dig.*, 501 (1993).
15. J. G. Fossum, A. Ortiz-Conde, H. Shichijo, and S. K. Banerjee, *IEEE Trans. Electron Devices*, **ED-32,** 1878 (1985).
16. K. Fuse, Y. Sakata, T. Inoue, K. Yamauchi, and Y. Yatsuda, *Springer Proceedings in Physics*, Vol. 35, p. 370 (1989).

The Effect of Post-Cure Annealing on the Protective Properties of Polyimides on Chromium Substrates

D. B. Mitton and R. M. Latanision*

H. H. Uhlig Corrosion Laboratory, Massachusetts Institute of Technology, Cambridge, Massachusetts, 02139 USA

F. Bellucci*

Department of Materials and Production Engineering, University of Naples Federico II, P. Le Tecchio 80125, Naples, Italy

ABSTRACT

The effect of post-cure annealing on the protective properties of thin (2.6-2.8 μm) polyimide films on chromium metallic substrates was investigated in aerated neutral 0.05, 0.5, and 5 *M* aqueous NaCl solutions at ambient temperature (≈20°C). The study was carried out using the technique of electrochemical impedance spectroscopy to monitor film degradation as a function of immersion time in the test solutions. Results obtained indicate that when exposed to aqueous NaCl solutions for extended periods, a majority of the nonannealed coated substrates failed; however, the performance of the annealed samples was significantly better. At face value, these results suggested improved protective properties of the polyimide due to annealing. However, a more in-depth analysis of the data revealed that post-cure annealing leads to the development of a thicker oxide on the chromium substrate. The change in the oxide occurring during the post-cure annealing treatment contributes to the improved corrosion resistance of the polyimide/Cr system.

Introduction

To improve signal propagation speed and memory performance in microprocessors, device feature sizes in integrated circuits must be reduced to facilitate densification of microelectronics packages. Exposing such systems to aggressive processing and service environments can pose serious corrosion and reliability problems. Therefore, to ensure prolonged performance life and reliability, stringent demands are placed on packaging materials. Although the ability to planarize substrate surfaces, thermal stability, chemical resistance, and dielectric properties of polyimides favorably meet the requirements of such materials, the critical issue of corrosion protection is less well documented.[1-5] Additionally, polyimides are susceptible to the uptake of water and wet polyimides exhibit higher levels of conductivity than those recorded for the dry polymer.[6] Permeation of water and subsequently dissolved oxygen and ionic contaminants can alter mechanical[3] and electrical properties of devices leading to early failure.[2-5]

Recently, the protective properties of pyromellitic dianhydride oxidianiline (PMDA-ODA) polyimide coated on an Al metallic substrate,[1] have been investigated. This paper showed that the time to failure for a 2.4 μm PMDA-ODA polyimide on an aluminum substrate immersed in 0.5 *M* NaCl varied between a few days and 90 days. Early failure of samples has so far been interpreted in terms of defects, or pinholes, in the polymer. Conversely, failure observed after extended exposure to the environment was attributed to the loss of adhesion at the polymer-metal interface.

To improve the protection of a metallic substrate by a polymer such as polyimide, two aspects should be considered: (*i*) improving the adhesion at the polymer-metal interface and (*ii*) reducing the preexisting heterogeneities within the polymer, which may result from unreleased trapped solvent or unreacted polyamic acid. The first issue is addressed in this paper by employing a chromium metallic substrate. It has been demonstrated that adhesion between polyimide and Cr is better than between polyimide and other metals such as Al and Cu.[7] In order to reduce the number of preexisting heterogeneities in the current study, a post-cure anneal was instituted. When this treatment is carried out at a temperature close to T_g, removal of the residual high boiling point solvents (*e.g.*, dimethylacetamide, DMA, and n-methylpyrrolidone, NMP) should reduce the number of preexisting heterogeneities. In addition, this post-cure thermal treatment will allow the complete curing of unreacted polyimides which are known to be present in polyimide films and can be as high as 20%.[8]

In order to extend our understanding of the protective properties of polyimides, this paper reports an experimen-

* Electrochemical Society Active Member.